Relaxation and spectral line shape in Fourier transform ion resonance spectroscopy[a)]

Alan G. Marshall,[b),c)] Melvin B. Comisarow,[b)] and Gérald Parisod

Department of Chemistry, University of British Columbia, Vancouver, B.C. V6T 1W5 Canada
(Received 18 January 1979)

Analytical expressions for Fourier transform ion cyclotron resonance (FT-ICR) line shape [absorption mode, dispersion mode, and magnitude (absolute value) mode] are derived for coherently excited ions that undergo both reactive and nonreactive ion–molecule collisions. The expressions are valid at arbitrary sample pressure, and reduce to particularly simple form in the "zero-pressure" limit (essentially no ion–molecule collisions during the data acquisition period) or "high-pressure" limit (many ion–molecule collisions during the data acquisition period). The zero-pressure line shape has been analyzed in earlier papers; in this paper, various useful properties of the high-pressure line shape (e.g., linewidth, mass resolution, and upper mass limit) are tabulated for various choices of the fraction of maximal absorption (or magnitude) peak height at which linewidth is to be measured. Absorption, dispersion, and magnitude spectra are plotted for zero-pressure and high-pressure limits, and also for an intermediate pressure. Convenient reference graphs of high-pressure FT-ICR linewidth, mass resolution, and upper mass limit as functions of ionic mass and time-domain ICR half-life for singly charged ions at magnetic field strength of 2 T are included. Finally, the intermediate-pressure resolution is calculated as a function of acquisition period at fixed pressure, to shown that near-optimal mass resolution (to within 90% of maximal absorption-mode resolution, or 95% of maximal magnitude-mode resolution) is achieved by truncating the FT-ICR time-domain signal after just three relaxation times. Good agreement between experimental and theoretical line shape (and thus mass resolution) is demonstrated.

I. INTRODUCTION

In a previous paper,[1] the fundamental relationships for linewidth and resolution for all forms of ion cyclotron resonance spectroscopy were derived. Mass resolution and frequency resolution were shown to be numerically identical in all forms of ion cyclotron resonance spectroscopy. The theoretical Fourier transform ion cyclotron resonance (FT-ICR) spectral line shape was then calculated for the *low-pressure limit*, in which there are essentially no ion–molecule collisions during the observation period. Absorption, dispersion, and magnitude (absolute-value) line shapes were illustrated and discussed. FT-ICR linewidth, resolution, and upper mass limit were expressed as functions *either* of ionic charge, applied magnetic field strength, and data acquisition time, *or* of computer data storage size and minimum specified ionic mass in the FT-ICR mass range, and the results tabulated for several linewidth criteria. The principal low-pressure FT-ICR line shape properties are collected, along with several convenient graphical plots summarizing the dependence of FT-ICR low-pressure resolution and upper ionic mass limit on ionic mass and observation time, in a recent review.[3]

In the second paper in this series,[2] the origin of the FT-ICR signal was discussed. The excited ICR system was modeled as a rotating electric monopole that gives rise to the FT-ICR signal. Unlike prior ICR signal models, the rotating monopole signal model is applicable to all ICR spectrometers that use radiofrequency detection methods and readily explains the presence of an ICR signal in the absence of an alternating electric field. The ICR signal strength was derived as a function of instrumental parameters such as number of ions, magnetic field strength, ICR cell dimensions, etc. Formulas were derived for the damping of the ICR motion due to resistive heating in the external circuit used for monitoring the signal. Comparisons were made between the rotating electric monopole model and the signal generating models used in other coherent radiation spectroscopies such as NMR and microwave spectroscopy.

The present paper presents an extension of the theory of Part I[1] to the important general case that ion–molecule collisions affect the FT-ICR line shape. The FT-ICR spectral line shape is first derived for ions which undergo an *arbitrary* number of ion–molecule collisions (reactive and nonreactive) during the data acquisition period. The analytical absorption, dispersion, and magnitude (absolute-value) line shapes are tabulated and also illustrated graphically, showing simple limiting behavior either at very *low pressure* (essentially no ion–molecule collisions during the observation period) or at very *high pressure* (a given ion undergoes many collisions during the acquisition period). By appropriate choice of data acquisition time T, one or the other of these limiting conditions will apply: The *zero-pressure* case has been treated at length in Refs. 1 and 3, while most of this paper is devoted to quantitative analysis of the *intermediate* and *high-pressure* line shape. Various useful tabulations and graphs are presented and discussed.

II. SUMMARY OF GENERAL EQUATIONS FOR ICR FREQUENCY, LINEWIDTH, RESOLUTION, AND UPPER MASS LIMIT

Equations (1)–(5) have been derived and discussed in earlier papers[1,3]:

$$\omega = \frac{qB}{m} , \tag{1a}$$

where q is the ionic charge in C, B is the applied static

[a)] "Theory of Fourier Transform Ion cyclotron Resonance Mass Spectroscopy III." Part I, Ref. 1; Part II, Ref. 2.
[b)] Author to whom correspondence may be addressed.
[c)] Alfred P. Sloan Research Fellow, 1976–80.

 0021-9606/79/234434-11$01.00

magnetic field in T, m is the ionic mass in kg, and ω is the ion cyclotron resonant frequency in (rad) sec^{-1};

$$\omega = 9.645 \times 10^6 \frac{qB}{m} , \tag{1b}$$

with q in multiples of electronic charge, B in kG, m in a. m. u., and ω in (rad) sec^{-1};

$$\nu = 1.535 \times 10^6 \frac{qB}{m} , \tag{1c}$$

with q in multiples of electronic charge, B in kG; m in a. m. u., and ν in Hz;

$$\frac{\omega}{\Delta\omega} = \frac{m}{\Delta m} , \tag{2}$$

with ω and $\Delta\omega$ in the same (arbitrary) units, m and Δm in the same (arbitrary) units, and $\Delta\omega$ and Δm are frequency and mass increments, respectively, (see text);

$$\Delta m = \left(\frac{m^2}{qB}\right)\Delta\omega , \tag{3a}$$

with q in C, B in T, m and Δm in kg, and $\Delta\omega$ in (rad) sec^{-1};

$$\Delta m = 1.037 \times 10^{-7}\left(\frac{m^2}{qB}\right)\Delta\omega , \tag{3b}$$

with q in multiples of electronic charge, B in kG, m and Δm in a. m. u., and $\Delta\omega$ in (rad) sec^{-1};

$$\frac{m}{\Delta m} = \frac{qB}{m\Delta\omega} , \tag{4a}$$

with q in C, B in T, m and Δm in kg, and $\Delta\omega$ in (rad) sec^{-1};

$$\frac{m}{\Delta m} = 9.645 \times 10^6 \frac{qB}{m\Delta\omega} , \tag{4b}$$

with q in multiples of electronic charge, B in kG, m and Δm in a. m. u., $\Delta\omega$ in (rad) sec^{-1};

$$m_{max} = \sqrt{\frac{qB\Delta m}{\Delta\omega}} , \tag{5a}$$

with q in C, B in T, m_{max} and Δm in kg, and $\Delta\omega$ in (rad) sec^{-1};

$$m_{max} = 3.106 \times 10^3 \sqrt{\frac{qB\Delta m}{\Delta\omega}} , \tag{5b}$$

with q in multiples of electronic charge, B in kG, m_{max} and Δm in a. m. u., and $\Delta\omega$ in (rad) sec^{-1}.

Equation (1) is the fundamental equation for orbital ion motion in a static magnetic field.[4] Equation (2) states that resolution defined for the *frequency* scale $\omega/\Delta\omega$ is numerically identical to resolution defined for the *mass* scale $m/\Delta m$. Equations (3) and (4) are the general expressions for ICR mass increment Δm and (mass) resolution $m/\Delta m$ for a given frequency increment $\Delta\omega$. In our applications, $\Delta\omega$ will be defined as the width of an ICR frequency-domain response, measured at a specified fraction of the frequency-domain peak height. Finally, Eq. (5) gives the upper mass limit m_{max} in terms of the maximum desired mass increment Δm for a particular (independently specified) frequency increment $\Delta\omega$ (see below).

It is to be emphasized that Eqs. (1)–(5) are valid for *any* ion cyclotron resonance spectrometer (e. g., magnetic field-sweep,[5,15] frequency-sweep,[6,7] FT-ICR[1-3,8-14]) for *any* arbitrary definition of frequency or mass increment. These equations form the basis for subsequent analytical and tabular expressions for conventional ICR or FT-ICR spectral linewidth, (mass) resolution, and upper mass limit.

III. THEORY: ANALYTICAL EXPRESSIONS FOR THE ICR LINE SHAPE

A. Line shape for "drift" cell and "trapped-ion" cell spectrometers

It has previously been noted that any process that interrupts coherent ion cyclotron orbital motion contributes to broadening of the ICR frequency-domain response.[11] In conventional ("drift"[5,15] or "trapped-ion"[16]) ICR spectrometers, the ICR frequency-domain response is determined from power absorption measurements,[2,17,18] so that ions are irradiated continuously *during* the detection. Thus, ions that are removed by ion–molecule *reactions* cease to contribute to power absorption after reaction, while ions that undergo *nonreactive* ion–molecule *collisions* begin to absorb power again immediately after a collision. In summing up the total power absorption from all ions in a sample, it is therefore necessary to distinguish between reactive and nonreactive collisions, and the resultant expression for frequency-domain response can become quite complicated.[17,18] For primary ions, for example, power absorption from a conventional drift or trapped ion spectrometer is given by Eq. (6)[18]:

$$P(\omega') \propto \frac{1}{\xi^2 + (\omega - \omega')^2}\left(\left\{\frac{[\xi(k+\xi) - (\omega-\omega')^2]\cos[(\omega-\omega')T] - (\omega-\omega')(2\xi+k)\sin[(\omega-\omega')T]}{(\xi+k)^2 + (\omega-\omega')^2}\right\}\exp[-(\xi+k)T]\right.$$
$$\left. - \frac{\xi(\xi+k) - (\omega-\omega')^2}{(\xi+k)^2 + (\omega-\omega')^2} - \frac{\xi}{k}[\exp(-kT) - 1]\right) , \tag{6}$$

in which k is the (first-order) rate constant for (exponential) disappearance of reactive ions due to ion–molecule reactions, ξ is the reduced collision frequency, T is the drift period (for a drift cell) or the trapping period (for a trapped-ion cell), ω' is the frequency at which power absorption is measured, and ω is the ion cyclotron resonant frequency given by Eq. (1). k is thus a measure of the rate at which ions are removed from the sample by ion–molecule *reactions*, while ξ is a measure of the average rate at which ion velocity is reduced due to nonreactive ion–molecule *collisions*.[6,15,18]

Although the general line shape of Eq. (6) is complicated, its behavior becomes simple under two types of

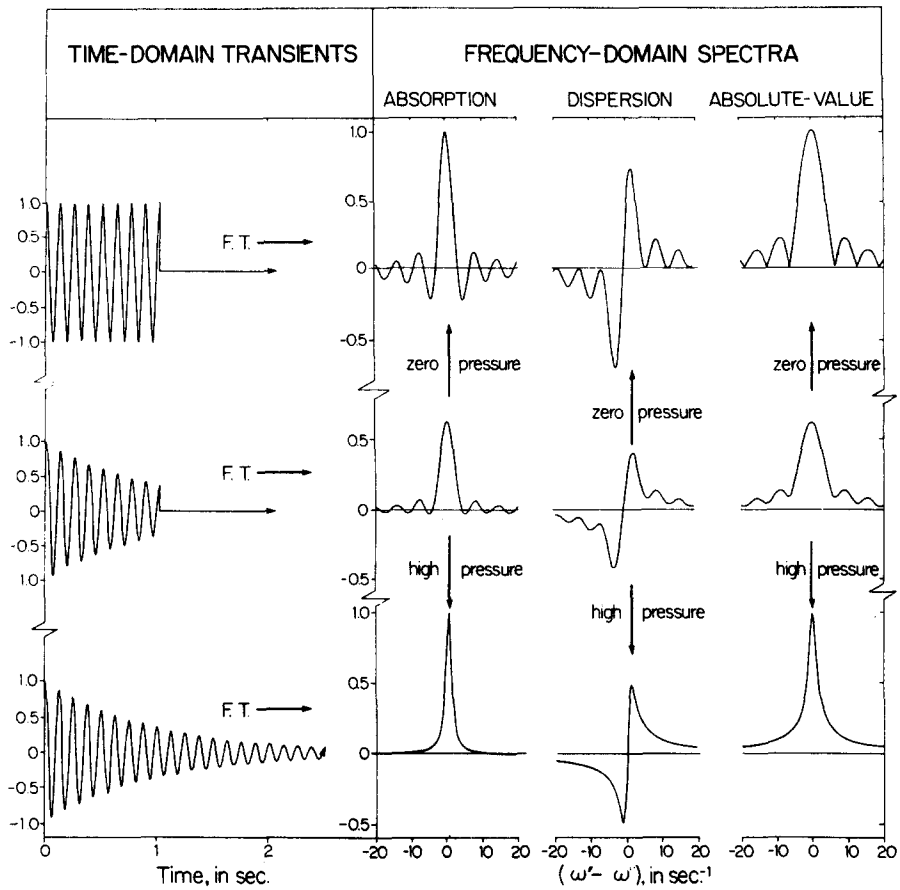

FIG. 1. Cosine transform (absorption), sine transform (dispersion), and magnitude (absolute-value) frequency-domain ICR spectra obtained by analytical Fourier transformation of the continuous time-domain signals shown at the left of each set of spectra. The spectra are computed from the general FT-ICR line shape expressions in Table I; all frequency-domain spectra have the same horizontal and vertical scale. The top row of graphs corresponds to the zero-pressure limit ($T \ll \tau$), the bottom row to the high-pressure limit ($T \gg \tau$), and the middle row to an intermediate pressure for which $T = \tau$, where T is the data acquisition period and τ is the relaxation time for (expotential) decay of the FT-ICR time-domain signal.

limiting conditions. First, in the "zero-pressure" limit that there are essentially no ion–molecule collisions during the observation period T,

$$\lim_{k,\xi \to 0} P(\omega') \propto \frac{1-\cos[(\omega-\omega')T]}{(\omega-\omega')^2}$$

$$= \text{zero-pressure line shape for conventional ICR} . \tag{7}$$

Alternatively, in the "high-pressure" limit that there are many ion–molecule collisions during the observation period T, Eq. (6) quickly reduces to

$$\lim_{\substack{\xi \gg (1/T), \\ k \ll \xi, (1/T)}} P(\omega') \propto \left[\frac{\xi}{\xi^2+(\omega-\omega')^2}\right] T$$

$$= \text{high-pressure line shape for conventional ICR (nonreactive primary ions)} . \tag{8}$$

Equations (6)–(8) are discussed in detail in Ref. 18. The conventional ICR high-pressure nonreactive primary ion line shape of Eq. (8) has the same form as the high-pressure (reactive *or* nonreactive) FT-ICR line shape discussed in detail in Sec. IV. The low-pressure conventional and FT-ICR line shapes have been treated at length in Refs. 1 and 3.

B. Line shape for FT-ICR spectrometers

In the FT-ICR experiment, a gaseous sample containing ions having a range of mass-to-change ratios is first subjected to a broadband frequency excitation. The excitation is then removed, and the signal induced[2] in the transverse (to the applied magnetic field) plates of the ICR cell by excited ICR coherent orbital motion may be taken as (Fig. 1, center left)

$$f(t) = 0 , \qquad t<0 \text{ or } t>T , \tag{9}$$

$$f(t) = KN(t)\exp(-\xi t)\cos(\omega t) , \qquad 0 \le t \le T , \tag{10}$$

in which K is a constant, $N(t)$ is the time-varying number of ions of ion cyclotron frequency ω, and ξ is the reduced collision frequency. The exponential term in Eq. (10) represents a decrease in the coherent ICR motion, due to nonreactive ion–molecule collisions. If k is the (first-order) rate constant for ion–molecule reactions, then the number of ions $N(t)$ also decreases exponentially according to

$$N(t) = N_0 \exp(-kt) , \tag{11}$$

in which N_0 is the number of coherently orbiting excited ions initially present at time zero (i.e., the beginning of the observation period). Combining Eqs. (10) and (11) gives

$$f(t) = KN_0 \exp(-t/\tau)\cos(\omega t) , \qquad 0 \le t \le T , \tag{12}$$

in which

$$(1/\tau) = \xi + k . \tag{13}$$

τ is the "overall relaxation time" for decay of the excited ICR signal due to reactive and nonreactive ion–molecule collisions.

Equation (10) [or (12)] will apply for reactive or non-

reactive ions. In the most general case, the time-domain signal $f(t)$ will consist of a sum of exponentially damped sinusoids when the ICR sample contains ions of various mass-to-charge ratios:

$$f(t)=\sum_i KN_{t_0}\exp(-t/\tau_i)\cos(\omega_i t)\ . \tag{14}$$

The amplitudes of the frequency components of $f(t)$, namely, $A(\omega')$ and $B(\omega')$ in

$$f(t)=\int_0^\infty A(\omega')\cos(\omega' t)d\omega'+\int_0^\infty B(\omega')\sin(\omega' t)\,d\omega'\ , \tag{15}$$

are obtained from the basic formulas for Fourier transforms

$$A(\omega')=\frac{1}{\pi}\int_0^\infty f(t)\cos(\omega' t)\,dt\ , \tag{16}$$

and

$$B(\omega')=\frac{1}{\pi}\int_0^\infty f(t)\sin(\omega' t)\,dt\ . \tag{17}$$

It will also prove of interest to consider the "magnitude" or "absolute-value" spectrum

$$C(\omega')=\{[A(\omega')]^2+[B(\omega')]^2\}^{1/2}\ . \tag{18}$$

A final frequency response $[C(\omega')]^2$ is called the "power" spectrum, and will not be considered further here.

By use of the trigonometric identities

$$\cos(X)\cos(Y)=(1/2)[\cos(X-Y)+\cos(X+Y)] \tag{19}$$

and

$$\sin(X)\cos(Y)=(1/2)[\sin(X-Y)+\sin(X+Y)]\ , \tag{20}$$

the evaluation of $A(\omega')$ and $B(\omega')$ is readily accomplished from the integrals

$$\int\exp(at)\cos(bt)\,dt=\frac{\exp(at)}{a^2+b^2}[a\cos(bt)+b\sin(bt)]\ , \tag{21}$$

and

$$\int\exp(at)\sin(bt)\,dt=\frac{\exp(at)}{a^2+b^2}[a\sin(bt)-b\cos(bt)]\ , \tag{22}$$

evaluated between the limits $t=0$ to $t=T$.

Analytical expressions for the absorption-mode and magnitude-mode spectra of Eqs. (16) and (18), based on the general time-domain ICR response of Eq. (12), are given below:

$$A(\omega')=\frac{(KN_0/2\pi)\tau}{1+(\omega-\omega')^2\tau^2}\times(1+\exp(-T/\tau)\{(\omega-\omega')\tau\sin[(\omega-\omega')T]-\cos[(\omega-\omega')T]\})\ , \tag{23}$$

$$C(\omega')=\frac{(KN_0/2\pi)\tau}{[1+(\omega-\omega')^2\tau^2]^{1/2}}\times\{1-2\exp(-T/\tau)\cos[(\omega-\omega')T]+\exp(-2T/\tau)\}^{1/2}\ . \tag{24}$$

Under the very general condition that the system response amplitude be proportional to the amplitude of the (applied oscillating electric field) excitation (i. e., that the system be "linear"), Eqs. (23) and (24) obtained via the cosine and sine Fourier transforms of Eqs. (16) and (17), respectively, are identical to the instantaneous steady-state power absorption and magnitude line shapes that would be obtained after the same observation period, T.[19] Analytical expressions for general and limiting forms of the absorption-, dispersion-, and magnitude-mode normalized line shapes are collected in Table I, along with other useful spectral properties (peak height and linewidth) for the limiting cases (see Sec. III B 1 and III B 2).

The time-domain signals and corresponding FT-ICR spectra for zero-pressure ($T\ll\tau$), high-pressure ($\tau\ll T$), and a particular intermediate ($T=\tau$) pressure are shown graphically in Fig. 1. The top row of graphs relates to a system at very low pressure with finite observation period T. The middle row of graphs relates to a system at intermediate (and experimentally typical) operating pressure for the same finite observation period T. The bottom row of graphs relates to a system at the same pressure, but with infinitely long observation period. The principal qualitative features of these spectra are (1) the auxiliary peaks on either side of the zero-pressure absorption-mode maximum gradually disappear as the pressure is increased, and (2) the magnitude (absolute-value) spectral linewidth (rightmost plot in a given row) is broader than the corresponding absorption-mode linewidth (leftmost spectrum in the same row), by a factor ranging from 2 to $\sqrt{3}$ as one proceeds from the zero-pressure to the high-pressure limit, respectively. Finally, comparing the two spectral modes for which experimental phase correction is required, namely, $A(\omega')$ and $B(\omega')$, we see that, at any pressure, the dispersion spectrum $[B(\omega')]$ spreads over a wider range of frequency.

1. *Zero-pressure limit ($\tau\gg T$)*

As with the conventional ICR line shape,[17,18] the FT-ICR frequency-domain spectra take on especially simple form in either the low-pressure ($\tau\gg T$) or high-pressure ($\tau\ll T$) limits. It may readily be verified that, for the low-pressure limit, the absorption-mode and magnitude-mode expressions of Eqs. (23) and (24) reduce to

$$\lim_{\tau\gg T}A(\omega')=(KN_0/2\pi)\frac{\sin[(\omega-\omega')T]}{(\omega-\omega')} \tag{25}$$

and

$$\lim_{\tau\ll T}C(\omega')=\frac{(KN_0/2\pi)\sqrt{2}}{(\omega-\omega')}\{1-\cos[(\omega-\omega')T]\}^{1/2}\ . \tag{26}$$

The low-pressure limiting line shapes of Eqs. (25) and (26) have been analyzed in detail in Refs. 1 and 3. They represent the Fraunhofer[20] line shape common to many physical phenomena.

2. *High-pressure limit ($\tau\ll T$)*

The FT-ICR Lorentz[20] absorption-mode and magnitude-mode analytical line shapes for the high-pressure limit ($\tau\ll T$), in which T is data acquisition period and is given by Eq. (13), are readily obtained from Eqs. (23) and (24) as

TABLE I. Summary of the FT-ICR line shape formulas and their principal properties, based on a time-domain signal which has the form $f(t) = \exp(-t/\tau)\cos(\omega t)$ between $t = 0$ and $t = T$, and is zero elsewhere.

	General formula[a]	Limiting formula	$\lim f(\omega')$ $(\omega - \omega') \to 0$	Frequency-scale linewidth at half-maximum height $\Delta\omega_{50\%}$
Absorption-mode	$A(\omega') = \frac{\tau}{1+(\omega-\omega')^2\tau^2}\,(1+\exp(-T/\tau)\{(\omega-\omega')\tau\sin[(\omega-\omega')T]-\cos[(\omega-\omega')T]\})$	Zero-pressure, $T \ll \tau$: $A(\omega') = \frac{\sin[(\omega-\omega')T]}{\omega-\omega'}$	T	$3.791/T$
		High-pressure, $T \gg \tau$: $A(\omega') = \frac{\tau}{1+(\omega-\omega')^2\tau^2}$	τ	$2/\tau$
Dispersion-mode	$B(\omega') = \frac{\tau}{1+(\omega-\omega')^2\tau^2}\,((\omega-\omega')\tau-\exp(-T/\tau)\{(\omega-\omega')\tau\cos[(\omega-\omega')T]+\sin[(\omega-\omega')T]\})$	Zero-pressure, $T \ll \tau$: $B(\omega') = \frac{1-\cos[(\omega-\omega')T]}{\omega-\omega'}$	$\pm(0.7246/T)$[b]	$4.662/T$[c]
		High-pressure, $T \gg \tau$: $B(\omega') = \frac{(\omega-\omega')\tau^2}{1+(\omega-\omega')^2\tau^2}$	$\pm\tau/2$	$2/\tau$
Magnitude-mode	$C(\omega') = \left[\frac{\tau^2}{1+(\omega-\omega')^2\tau^2}\right]^{(1/2)}\{1-2\exp(-T/\tau)\cos[(\omega-\omega')T]+\exp(-2T/\tau)\}^{1/2}$	Zero-pressure, $T \ll \tau$: $C(\omega') = \frac{\sqrt{2}}{\lvert\omega-\omega'\rvert}\{1-\cos[(\omega-\omega')T]\}^{1/2}$	T	$7.582/T$
		High-pressure, $T \gg \tau$: $C(\omega') = \frac{\tau}{[1+(\omega-\omega')^2\tau^2]^{1/2}}$	τ	$2\sqrt{3}/\tau$

[a] The scaling coefficient $(KN_0/2\pi)$ has been omitted.
[b] These are the extrema of $B(\omega')$, located at $(\omega-\omega') = \pm(2.331/T)$ and $(\omega-\omega') = \pm\tau/2$ for zero and high-pressure, respectively.
[c] The value represents the distance between the extrema of $B(\omega')$ on either side of $\omega' = \omega$.

TABLE II. FT-ICR linewidth and resolution formulas for the absorption-mode and magnitude (absolute-value) high-pressure line shape.

Spectral mode	Absorption = $A(\omega') = (K/2\pi)\frac{\tau}{1+(\omega-\omega')^2\tau^2}$					Magnitude (absolute-value) = $C(\omega') = (K/2\pi)\frac{\tau}{\sqrt{1+(\omega-\omega')^2\tau^2}}$				
Percentage of maximum peak height at which the linewidth is defined =	50%	25%	10%	5%	1%	50%	25%	10%	5%	1%
Frequency-scale linewidth $\Delta\omega$[(rad) sec^{-1}] =	$\frac{2.000}{\tau}$	$\frac{3.464}{\tau}$	$\frac{6.000}{\tau}$	$\frac{8.718}{\tau}$	$\frac{19.90}{\tau}$	$\frac{3.464}{\tau}$	$\frac{7.746}{\tau}$	$\frac{19.90}{\tau}$	$\frac{39.95}{\tau}$	$\frac{200.0}{\tau}$
Mass-scale linewidth[a] Δm (kg) =	$\frac{2.000\ m^2}{qB\tau}$	$\frac{3.464\ m^2}{qB\tau}$	$\frac{6.000\ m^2}{qB\tau}$	$\frac{8.718\ m^2}{qB\tau}$	$\frac{19.90\ m^2}{qB\tau}$	$\frac{3.464\ m^2}{qB\tau}$	$\frac{7.746\ m^2}{qB\tau}$	$\frac{19.90\ m^2}{qB\tau}$	$\frac{39.95\ m^2}{qB\tau}$	$\frac{200.0\ m^2}{qB\tau}$
Mass-scale linewidth[b] Δm (a. m. u.) =	$\frac{2.07\times10^{-4}\ m^2}{qB\tau}$	$\frac{3.59\times10^{-4}\ m^2}{qB\tau}$	$\frac{6.22\times10^{-4}\ m^2}{qB\tau}$	$\frac{9.04\times10^{-4}\ m^2}{qB\tau}$	$\frac{2.06\times10^{-3}\ m^2}{qB\tau}$	$\frac{3.59\times10^{-4}\ m^2}{qB\tau}$	$\frac{8.03\times10^{-4}\ m^2}{qB\tau}$	$\frac{2.06\times10^{-3}\ m^2}{qB\tau}$	$\frac{4.14\times10^{-3}\ m^2}{qB\tau}$	$\frac{2.07\times10^{-1}\ m^2}{qB\tau}$
FT-ICR resolution[a] $(m/\Delta m) = (\omega/\Delta\omega)$ =	$\frac{0.5000\ qB\tau}{m}$	$\frac{0.2887\ qB\tau}{m}$	$\frac{0.1667\ qB\tau}{m}$	$\frac{0.1147\ qB\tau}{m}$	$\frac{0.0503\ qB\tau}{m}$	$\frac{0.2887\ qB\tau}{m}$	$\frac{0.1291\ qB\tau}{m}$	$\frac{0.0503\ qB\tau}{m}$	$\frac{0.0250\ qB\tau}{m}$	$\frac{0.0050\ qB\tau}{m}$
FT-ICR resolution[b] $(m/\Delta m) = (\omega/\Delta\omega)$ =	$\frac{4.82\times10^{3}\ qB\tau}{m}$	$\frac{2.78\times10^{3}qB\tau}{m}$	$\frac{1.61\times10^{3}qB\tau}{m}$	$\frac{1.11\times10^{3}qB\tau}{m}$	$\frac{4.85\times10^{2}qB\tau}{m}$	$\frac{2.78\times10^{3}qB\tau}{m}$	$\frac{1.25\times10^{3}qB\tau}{m}$	$\frac{4.85\times10^{2}qB\tau}{m}$	$\frac{2.41\times10^{2}qB\tau}{m}$	$\frac{4.82\times10^{1}qB\tau}{m}$

[a] In these expressions, m is the ionic mass in kg, q is the ionic charge in C, B is the magnetic field strength in T, and τ is the time constant (in s) for exponential decay of the time-domain excited ICR signal.

[b] In these expressions, m is the ionic mass in a. m. u., q is the ionic charge in multiples of electronic charge, B is the magnetic field strength in kG, and τ is the time constant (in ms) for exponential decay of the time-domain excited ICR signal.

$$\lim_{\tau\ll T} A(\omega') = \frac{(KN_0/2\pi)\tau}{1+(\omega-\omega')^2\tau^2}$$

(high-pressure absorption-mode), (27)

$$\lim_{\tau\ll T} C(\omega') = \frac{(KN_0/2\pi)\tau}{[1+(\omega-\omega')^2\tau^2]^{1/2}}$$

(high-pressure magnitude-mode). (28)

In order to compute the theoretical FT-ICR high-pressure mass resolution, it is necessary to define the *width* of the FT-ICR line, measured at a specified *fraction* of the maximal peak *height* for that spectral mode (compare Refs. 1 and 3). It is readily verified from the limiting expressions (27) and (28) that the linewidths [in frequency units of (rad) sec^{-1}] at various fractions of maximal peak height are those given in the top row of Table II, for absorption-mode and magnitude (absolute-value) mode line shapes, respectively. The corresponding linewidths in mass units are obtained from Eqs. (3a) and (3b) and appear as the second and third rows of Table II. Finally, FT-ICR resolution in either MKS units or common laboratory units is readily obtained from Eqs. (4a) and (4b), using the respective linewidth expressions above, to obtain the FT-ICR mass resolution expressions listed as rows 4 and 5 of Table II.

Table II thus lists formulas for the FT-ICR linewidth (mass-scale or frequency-scale) and resolution for both absorption-mode and magnitude-mode line shapes, for several common definitions of the percentage of maximum peak height at which the linewidth is to be measured. Since FT-ICR mass-scale linewidth increases as the square of ionic mass [Eq. (3) and Table II], it is clear that FT-ICR (mass) resolution must decrease with increasing ionic mass [Eq. (4) and Table II]. Thus, it becomes useful to calculate the *maximum* ionic mass-to-charge ratio for which the linewidth has increased to a specified (maximum) number of mass units, say, to 1 a. m. u. or less. The desired upper mass limit formulas are obtained from Eq. (5a) (MKS units) or Eq. (5b) (laboratory units), using the linewidth expressions from Table II, with the results listed in Table III. Finally, the experimentally convenient half-life $t_{1/2}$ for ICR time-domain signal disappearance is related to the relaxation time of Eq. (13) according to

$$t_{1/2} = [\log_e(2)]\tau = 0.693\tau . \quad (29)$$

IV. RESULTS AND DISCUSSION

A. High-pressure line shape

We begin by examining the functional dependence of FT-ICR *high-pressure* linewidth, resolution, and upper mass limit upon ionic mass m, ionic charge q, (fixed) magnetic field strength B, and time-domain FT-ICR signal relaxation time τ. First (as for the FT-ICR *zero*-pressure line shape[1,3]), the FT-ICR *high*-pressure linewidth (in mass units) increases as the square of ionic mass [Eq. (3), Table II, second or third rows)], so that FT-ICR high-pressure resolution is inversely proportional to mass [Eq. (4), Table II, fourth or fifth rows)]. Furthermore, as for the FT-ICR *zero*-pres-

TABLE III. FT-ICR upper mass limit formulas for high-pressure absorption-mode or magnitude (absolute-value) line shapes, for various choices of the fraction of maximal peak height at which the linewidth is measured, and for various choices of the maximum allowed mass-scale linewidth. In all expressions, q is the ionic charge in multiples of the electronic charge, B is the magnetic field strength in kG, and $\tau_{1/2}$ is the ICR time-domain signal half-life in ms.

Spectral mode		Absorption = $A(\omega')$		Magnitude (absolute-value) = $C(\omega')$	
Percentage of peak maximal height at which the linewidth is measured =		50%	25%	50%	25%
Upper mass limit m_{max} (in a. m. u.)	$m = 1$ a. m. u. at $m = m_{max} = 83.5\sqrt{qB\tau_{1/2}}$	$63.4\sqrt{qB\tau_{1/2}}$	$63.4\sqrt{qB\tau_{1/2}}$	$42.4\sqrt{qB\tau_{1/2}}$	
	$m = 0.5$ a. m. u. at $m = m_{max} = 59.0\sqrt{qB\tau_{1/2}}$	$44.8\sqrt{qB\tau_{1/2}}$	$44.8\sqrt{qB\tau_{1/2}}$	$30.0\sqrt{qB\tau_{1/2}}$	
	$m = 0.25$ a. m. u. at $m = m_{max} = 41.7\sqrt{qB\tau_{1/2}}$	$31.7\sqrt{qB\tau_{1/2}}$	$31.7\sqrt{qB\tau_{1/2}}$	$21.2\sqrt{qB\tau_{1/2}}$	
	$m = 0.1$ a. m. u. at $m = m_{max} = 26.4\sqrt{qB\tau_{1/2}}$	$20.0\sqrt{qB\tau_{1/2}}$	$20.0\sqrt{qB\tau_{1/2}}$	$13.4\sqrt{qB\tau_{1/2}}$	

sure linewidth (in mass units) is inversely proportional to the magnetic field strength (Table II, second or third rows), so that FT-ICR high-pressure resolution is directly proportional to magnetic field strength (Table II, fourth or fifth rows). Lastly, just as the *zero*-pressure FT-ICR linewidth is inversely proportional to the data acquisition time (with the result that *zero*-pressure FT-ICR resolution is directly proportional to data acquisition time), the FT-ICR *high*-pressure linewidth is inversely proportional to the FT-ICR time-domain relaxation time (or half-life) τ (or $t_{1/2}$).[21]

In summary, the larger the applied (fixed) magnetic field strength, the longer the data acquisition period, and the fewer the number of ion–molecule collisions and/or reactions during the acquisition time, the better the FT-ICR resolution. All these FT-ICR functional dependencies are shared by conventional ICR line shapes, although the proportionality constants in general differ from the FT-ICR case.[1]

The formulas from Table II for the FT-ICR high-pressure linewidth and resolution have been used to generate graphs showing the dependence of the FT-ICR high-pressure linewidth (in a. m. u.) on ionic mass (in a. m. u.) in Fig. 2, and of FT-ICR high-pressure resolution on either ionic mass in a. m. u. (Fig. 3) or on time-domain FT-ICR half-life (in ms) in Fig. 4, for singly charged ions in a typical magnetic field of 20 kG, for ionic masses and FT-ICR half-lives commonly encountered in actual experiments. Finally, Fig. 5 shows the dependence of the FT-ICR high-pressure upper mass limit m_{max} (in a. m. u.) on the FT-ICR time-domain half-life. In Figs. 2–5, the results for both absorption-mode and magnitude-mode line shapes are shown. Although absorption-mode resolution is better by a factor of $\sqrt{3}$, in the high-pressure limit, the magnitude mode

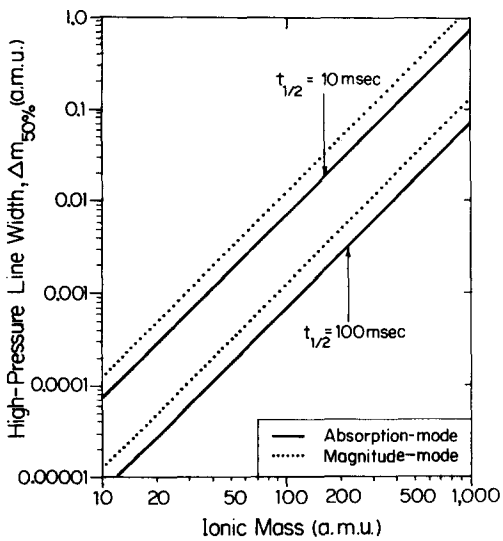

FIG. 2. Theoretical high-pressure FT-ICR linewidth Δm as a function of ionic mass for a magnetic field intensity $B = 20$ kG. Results are displayed for two choices of FT-ICR time-domain half-life, and are plotted for both absorption mode and magnitude (absolute-value) mode line shapes, The linewidth is measured at 50% of the maximum absorption (or magnitude) peak height, using the formulas in the first and sixth columns of the fourth row of Table II. The ions are singly charged.

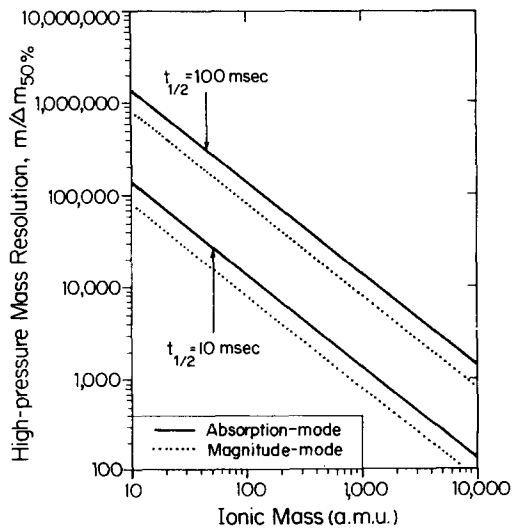

FIG. 3. Theoretical high-pressure FT-ICR (mass) resolution $m/\Delta m$ as a function of ionic mass for a magnetic field intensity $B = 20$ kG for singly charged ions. Results are shown for two choices of FT-ICR time-domain half-life, and are plotted for both absorption mode and magnitude mode line shapes. The linewidth is measured at 50% of the maximum absorption (or magnitude) peak height, using the formulas in the first and sixth columns of the sixth row of Table II.

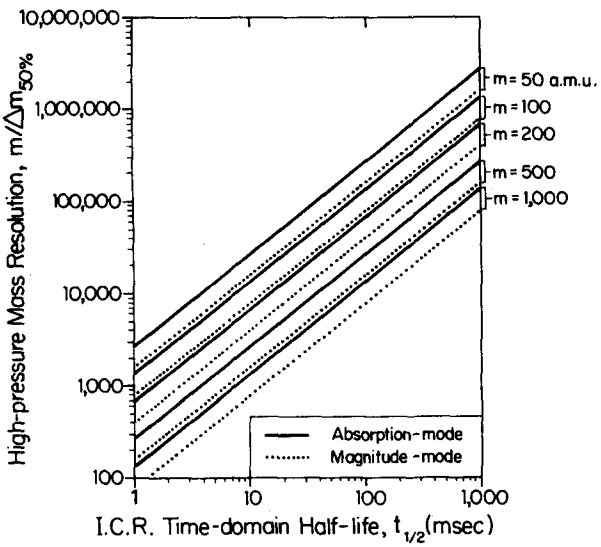

FIG. 4. Theoretical high-pressure FT-ICR (mass) resolution as a function of FT-ICR time-domain half-life for singly charged ions at a magnetic field strength $B = 20$ kG. Results are shown for several specific ionic masses, and are plotted for both absorption mode and magnitude mode line shapes. The linewidth is measured at 50% of the maximum absorption (or magnitude) peak height, with calculations based on the formulas in the first and sixth columns of the sixth row of Table II.

is often preferred, since no experimental phase correction is required.[10] The convention that the linewidth be measured at half the maximum absorption (or magnitude) peak height has been followed in Figs. 2–5; various other conventions are collected in Tables II and III for reference.

B. Intermediate-pressure line shape

The high-pressure [Eqs. (27) and (28)] and zero-pressure [Eqs. (25) and (26)] line shapes are obviously

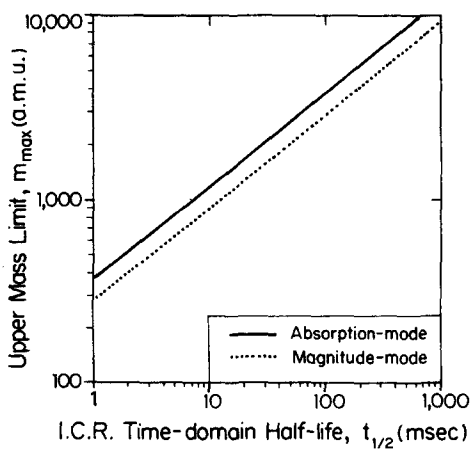

FIG. 5. Theoretical FT-ICR upper mass limit for the high-pressure line shape as a function of FT-ICR time-domain half-life for singly charged ions at a magnetic field strength $B = 20$ kG. Results are plotted for both absorption-mode and magnitude-mode line shapes, using the formulas in columns 1 and 3 of the first row of Table III. Upper mass limit is defined as the lowest mass at which the mass-scale linewidth has increased to 1.00 a.m.u., where the linewidth is measured at 50% of the maximum absorption (or magnitude) peak height.

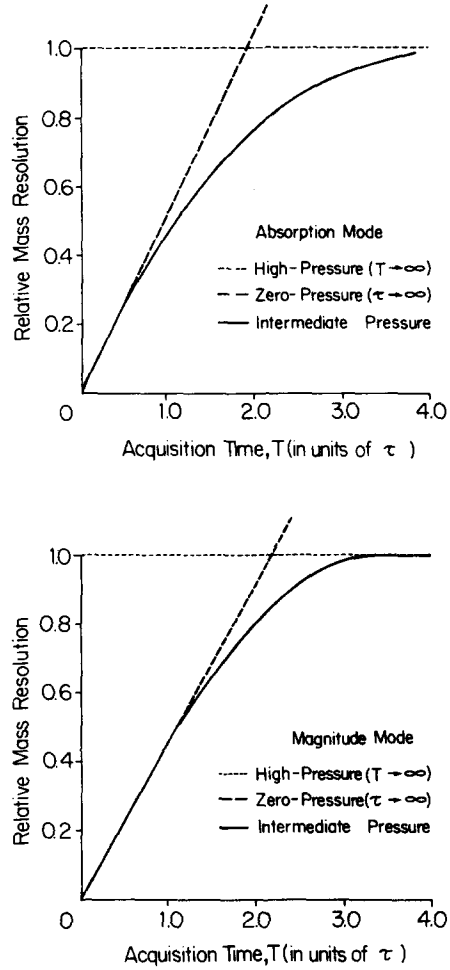

FIG. 6. Plots of relative FT-ICR theoretical mass resolution [from Eq. (24)] as a function of the ratio of data acquisition period T to the ICR time-domain relaxation time τ for either absorption-mode [Fig. 6(a)] or magnitude-mode [Fig. 6(b)] intermediate-pressure line shapes. The linewidth is measured at 50% of the maximal absorption (or magnitude) peak height. Relative mass resolution is obtained by dividing the mass resolution that would be obtained at that pressure using an infinitely long data acquisition period by the mass resolution at the stated acquisition period (see text).

two extreme limits of the general or intermediate-pressure [Eqs. (23) and (24)] line shapes (Table I) that are encountered in actual FT-ICR experiments. At *any* pressure, the FT-ICR *linewidth* (in mass units) varies directly as the square of ionic mass, and inversely with applied magnetic field strength or ionic charge [Eq. (3)]. Thus, at *any* pressure, the FT-ICR *resolution* varies directly with ionic charge and applied magnetic field strength, and inversely with ionic mass [Eq. (4)].

Figure 6 shows plots of the intermediate-pressure FT-ICR relative (mass) resolution as a function of the ratio of data acquisition period (T) to ICR time-domain relaxation time (τ) for either the absorption-mode line shape [Fig. 6(a)] or magnitude-mode line shape [Fig. 6(b)], based on the measurement of the linewidth at 50% of the maximal peak height. Thus, if the sample pressure (and therefore τ) is fixed, Fig. 6 shows that FT-ICR resolution is maximized by using *longer* data

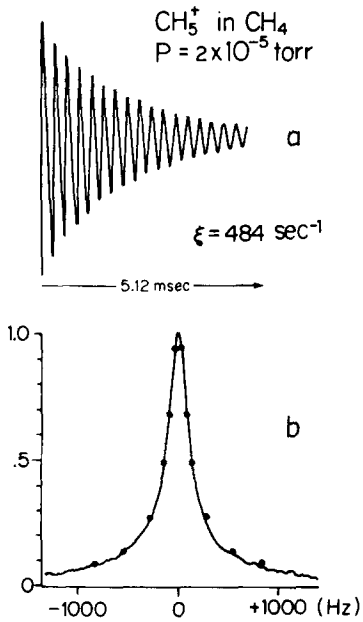

FIG. 7. Experimental FT-ICR transient signal (a) and magnitude-mode spectrum (b). A digitized FT-ICR transient signal from coherently excited CH_5^+ ions whose ICR motion is damped by collisions with neutral CH_4 molecules was acquired for 40.96 ms. Only the first 5.12 ms of the transient are shown in Fig. 7(a). The solid curve in Fig. 7(b) is the experimental magnitude-mode FT-ICR spectrum resulting from discrete Fourier transformation of the entire 40.96 ms digitized transient. The relaxation time τ is 2.1 ms, determined either by analysis of the exponential envelope of the time-domain transient or from the width at half-maximum height $\Delta\omega_{50\%} = 2\sqrt{3}/\tau$ of the magnitude-mode spectrum. Finally, the solid circles in Fig. 7(b) are the magnitude-mode spectral amplitudes calculated from Eq. (24) with $T = 40.96$ ms and $\tau = 2.1$ ms.

acquisition period. Figure 6 shows that after just three time-domain relaxation times, FT-ICR relative mass resolution has already increased to about 90% (absorption-mode) or 95% (magnetic-mode) of the limiting resolution that would be obtained for an infinitely long acquisition period. The trade-off between signal-to-noise ratio and mass resolution is discussed in Ref. 22.

C. Experimental confirmation of theory

Several aspects of the theory of the previous sections are susceptible to experimental test. The present experiments were performed on a homebuilt FT-ICR spectrometer described elsewhere,[23] and data were collected using the spectral segment extraction procedure.[3]

First, the formulas in Table II imply a simple theoretical relationship between the high-pressure linewidth in the frequency domain and the ICR relaxation time for the time-domain transient signal. Experimental confirmation of this relationship is given in Fig. 7. Figure 7(a) is a spectrally extracted FT-ICR transient (time-domain) signal from coherently excited CH_5^+ ions whose coherent ICR motion is damped by collisions with neutral CH_4 molecules. Although the CH_5^+ transient signal was acquired for 40.96 ms, only the first 5.12 ms are displayed in Fig. 7(a). Digital Fourier transformation of the entire 40.96 ms digitized transient gave the experimental magnitude-mode spectrum shown in Fig. 7(b). The relaxation time τ determined either from the exponential decay constant of the envelope of the time-domain transient [Fig. 7(a)], or from the formula (Table I)

$$\Delta\omega_{50\%} = (2\sqrt{3}/\tau) \tag{30}$$

applied to the spectrum of Fig. 7(b) is 2.1 ms. Furthermore, the solid circles in Fig. 7(b) represent magnitude-mode spectral amplitudes at selected frequencies, calculated from the high-pressure line shape of Eq. (28). These calculated spectral amplitudes are clearly in excellent agreement with the experimental spectrum, confirming that the full line shape (not just the magnitude-mode linewidth) is accurately represented by the theory.

Figure 7 affords experimental confirmation of the *high-pressure* FT-ICR line shape; the *intermediate-pressure* line shape may now be tested from the dependence of the magnitude-mode FT-ICR line shape upon the data acquisition period at fixed sample pressure, based on the high-resolution spectra of a mixture of HNO^- and CH_3O^- shown in Fig. 8. These ions are

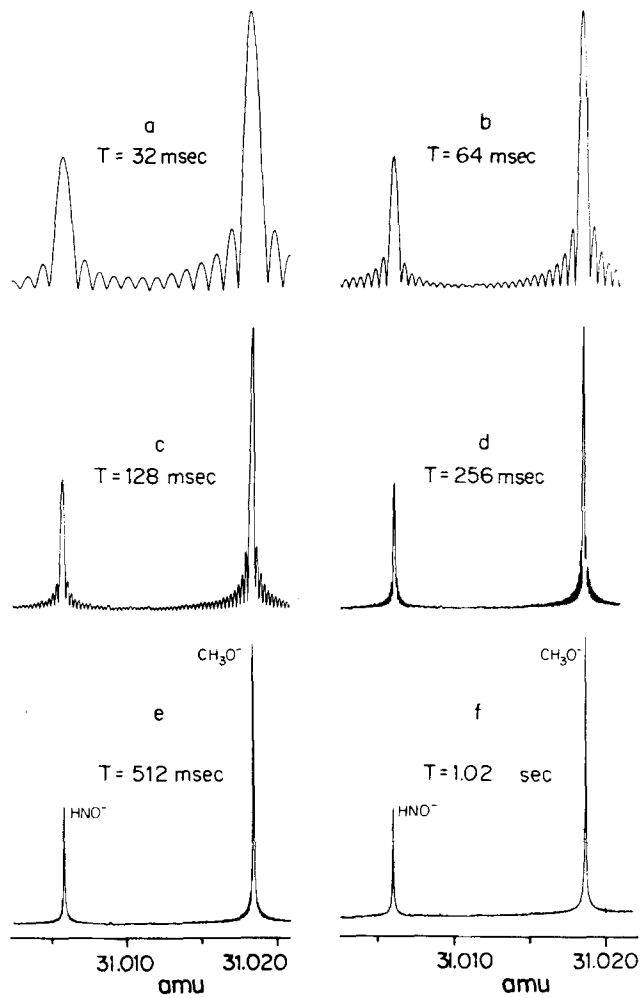

FIG. 8. Experimental FT-ICR magnitude-mode spectra of HNO^- and CH_3O^- as a function of data acquisition period. A time-domain transient ICR signal from HNO^- and CH_3O^- was digitized and acquired for periods T ranging from 32 ms [Fig. 8(a)] to 1.02 s [Fig. 8(f)]. The linewidths of the CH_3O^- spectra shown here provide the data for Fig. 9.

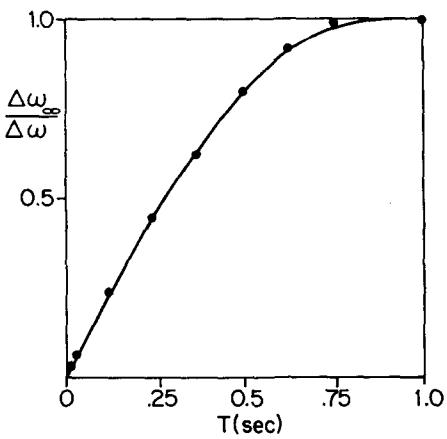

FIG. 9. Dependence of the experimental FT-ICR collision-broadened linewidth upon data acquisition period, at fixed sample pressure. A transient time-domain ICR signal from CH_3O^- ions in CH_3ONO was digitized and acquired for various periods, then Fourier transformed, and the linewidth at half-maximal magnitude-mode peak height determined (see Fig. 8). Each solid circle represents the ratio of the linewidth for the maximal acquisition period divided by the linewidth at the stated (shorter) acquisition period. The relaxation time determined from the linewidth for Fig. 8(f) is 250 ms. The solid curve is the theoretical relative mass resolution [from Eq. (24)] computed for $\tau = 0.25$ s and $0 \leq T \leq 1.02$ s (see text).

formed by impact of low energy electrons upon CH_3ONO.[24] After broadband excitation, the transient (time-domain) FT-ICR signal is eventually damped to zero by reactive[25] and nonreactive collisions with the neutral background gas. The various individual frequency-domain spectra in Fig. 8 resulted from discrete Fourier transformation of digitized transient signals that were acquired for different (indicated) acquisition periods. As the acquisition period progressively increases from 32 ms [Fig. 8(a)] to 1.02 s [Fig. 8(f)], the line shape progressively changes from the low-pressure form [Eq. (26)] to the high-pressure form [Eq. (28)]. For example, the experimental linewidth at half-maximal peak height for an acquisition period of 32 ms [38.2 Hz from Fig. 8(a)] is in excellent agreement with the theoretical linewidth of 38.0 Hz calculated from the zero-pressure limiting line shape of Eq. (26) with $T = 32$ ms.

Alternatively, a relaxation time of $\tau = 0.25$ s may be calculated from the experimental linewidth (2.2 Hz) at half-maximal peak height of the CH_3O^- peak in Fig. 8(f), using the high-pressure line shape of Eq. (28). From this τ value and the known acquisition periods T indicated in Figs. 8(a)–8(e), the relative experimental FT-ICR mass resolution may be calculated as a function of T. Figure 9 gives the result of this calculation. Each solid circle in Fig. 9 represents a ratio of the (high-pressure limiting) linewidth for the maximum (effectively infinite) acquisition period divided by the experimental linewidth for the indicated (shorter) acquisition period. The solid curve in Fig. 9 is the theoretical relative mass resolution [from Eq. (24)] calculated for $\tau = 0.25$ s and $0 \leq T \leq 1.02$ s. The experimental data points are in excellent agreement with the theory, demonstrating that Eq. (24) provides an accurate description of the experimental FT-ICR intermediate-pressure magnitude-mode line shape.

V. SUMMARY

Analytical expressions for FT-ICR frequency-domain spectra (absorption-mode, dispersion-mode, and magnitude-mode) have been derived for ions that may undergo both reactive and nonreactive ion–molecule collisions. Provided that the duration of the broadband FT-ICR excitation is short compared to all chemical (i.e., ion–molecule reaction) relaxation times, the analytical line shape for reactive and nonreactive ions is given simply by Eqs. (23) (absorption-mode) and (24) (magnitude-mode).

In contrast to the conventional ICR line shape, which is described by a very complicated function of reactive and nonreactive ion–molecule collision rate constants, and which exhibits completely different algebraic form for primary, secondary, and tertiary ions,[17,18] the FT-ICR high-pressure linewidth is simply proportional to the sum of the reactive and nonreactive reciprocal chemical relaxation times, and has the same functional form for both reactive and nonreactive ions. Thus, low-pressure FT-ICR spectra furnish high-resolution mass spectra for chemical applications,[1,3,11,14] while high-pressure FT-ICR spectra provide for particularly simple determinations of ion–molecule collision rate constants.[21]

Finally, the theoretical (Fig. 6) and experimental (Fig. 9) results in this paper demonstrate that the high-resolution capability inherent in FT-ICR can be realized in practice, while retaining most of the large signal-to-noise enhancement derived from the multichannel advantage[12,22] of Fourier data reduction.

ACKNOWLEDGMENTS

This work was supported by grants from the Natural Science and Engineering Research Council of Canada (MBC, AGM), the Research Corporation (MBC), and the Alfred P. Sloan Foundation (AGM).

[1] M. B. Comisarow and A. G. Marshall, J. Chem. Phys. **64**, 110 (1976).
[2] M. B. Comisarow, J. Chem. Phys. **68**, 4097 (1978).
[3] M. B. Comisarow, in *Transform Techniques in Chemistry*, edited by P. R. Griffiths (Plenum, New York, 1978), Chap. 10. (In Fig. 10.6 of this reference, the line labeled as $m = 100$ a.m.u. should be labeled $m = 50$ a.m.u.).
[4] E. O. Lawrence and M. S. Livingstone, Phys. Rev. **40**, 19 (1932).
[5] T. A. Lehman and M. M. Bursey, *Ion Cyclotron Resonance Spectrometry* (Wiley-Interscience, New York, 1976).
[6] D. Wobschall, Rev. Sci. Instrum. **36**, 466 (1965).
[7] R. L. Hunter and T. R. McIver, Jr., Am. Lab. **9**, 13 (1977).
[8] M. B. Comisarow and A. G. Marshall, Chem. Phys. Lett. **25**, 282 (1974).
[9] M. B. Comisarow and A. G. Marshall, Chem. Phys. Lett. **26**, 489 (1974).
[10] M. B. Comisarow and A. G. Marshall, Can. J. Chem. **52**, 1997 (1974).
[11] M. B. Comisarow and A. G. Marshall, J. Chem. Phys. **62**,

293 (1975).
[12]A. G. Marshall and M. B. Comisarow, in *Transform Techniques in Chemistry*, edited by P. R. Griffiths (Plenum, New York, 1978), Chap. 3.
[13]M. B. Comisarow, Adv. Mass Spectrom. 7, 1042 (1978).
[14]M. B. Comisarow, V. Grassi, and G. Parisod, Chem. Phys. Lett. **57**, 413 (1978).
[15]J. L. Beauchamp, Annu. Rev. Phys. Chem. **22**, 527 (1971).
[16]R. T. McIver, Jr., Rev. Sci. Instrum. **41**, 555 (1970).
[17]A. G. Marshall, J. Chem. Phys. **55**, 1343 (1971).
[18]M. B. Comisarow, J. Chem. Phys. **55**, 205 (1971).
[19]D. C. Champeney, *Fourier Transforms and their Physical Applications* (Academic, London, 1973), pp. 91–93.
[20]A. G. Marshall, *Biophysical Chemistry: Principles, Techniques and Applications* (Wiley, New York, 1978), Chaps. 13 and 20.
[21]G. Parisod and M. B. Comisarow, Chem. Phys. Lett. **62**, 303 (1979).
[22]A. G. Marshall, Anal. Chem. 51, 1710 (1979).
[23]M. Comisarow, G. Parisod, and V. Grassi, Proceedings of the 26th Annual Conference on Mass Spectrometry and Allied Topics (St. Louis, MO., 28 May–2 June, 1978), Paper WP12, p. 633 of published proceedings.
[24]K. Jaeger and A. Henglein, Z. Naturforsch. **220**, 700 (1967).
[25]R. Farid and T. B. McMahon, Int. J. Mass. Spectrom. Ion Phys. **27**, 163 (1978).